6), 2.82 (s, 2).

8-Benzoyl-2,2-dimethyl-4-formyl-1,4,8-triazaspiro[4.5]decane (15). Formic acetic anhydride[11] was generated by combining 1.52 g (14.9 mmol) of acetic anhydride and 0.705 g (15.2 mmol) of 99% formic acid in 4 mL of ether and stirring the solution at 55 °C for 2 h. The resulting solution was cooled to 0 °C and then slowly added to a stirred solution of 4.04 g (14.8 mmol) of crude **12** in 30 mL of CH_2Cl_2. After a 13-h stir at 25 °C, the reaction mixture was extracted with cold 10% Na_2CO_3 (2 × 15 mL). The aqueous extracts were combined and back-extracted with CH_2Cl_2. The combined CH_2Cl_2 solutions were dried (K_2CO_3) and concentrated to a brownish foam. The foam was dissolved in ethyl acetate and chromatographed over 20 g of silica gel. Elution with ethyl acetate gave crude **15** which was crystallized from ether–hexanes to give 2.84 g (64%) of **15**: mp 149–150 °C; NMR δ 1.29 (s, 6), 3.48 (s, 2), 8.38 (s, 1); IR ($CHCl_3$) 1657, 1628 cm^{-1}. Anal. Calcd for $C_{17}H_{23}N_3O_2 \cdot {}^1/_4H_2O$: C, 66.75; H, 7.74; N, 13.74. Found: C, 67.14; H, 7.61; N, 13.83.

8-Benzoyl-2,2-dimethyl-4-formyl-1,4,8-triazaspiro[4.5]decanyl-1-oxy (16). To a stirred solution of 2.02 g (6.70 mmol) of **15** in 100 mL of CH_2Cl_2 at 0 °C was added dropwise 2.13 g (10.5 mmol) of 85% *m*-chloroperoxybenzoic acid in 100 mL of CH_2Cl_2. The resulting solution began turning orange after 10 min, and the solution was allowed to stir at 25 °C overnight. The deep orange solution was concentrated to dryness, and the residue was dissolved in 1:1 ethyl acetate–hexanes and chromatographed over 60 g of silica gel. Elution with the same solvent gave an orange fraction which was concentrated to dryness, yielding 1.44 g (68%) of crude oily **16**. Crystallization from ethyl acetate–hexanes afforded 1.26 g (59%) of pure orange **16**: mp 118–119 °C; IR ($CHCl_3$) 1665, 1628 cm^{-1}; ESR ($CHCl_3$) three lines, a_N = 14.46 G. Anal. Calcd for $C_{17}H_{22}N_3O_2$: C, 64.54; H, 7.01; N, 13.28. Found: C, 64.21; H, 6.55; N, 12.92.

2,2-Dimethyl-1,4,8-triazaspiro[4.5]decyl-1-oxy (18). To a stirred solution (N_2) of 400 mg of **16** in 16 mL of MeOH was added 16 mL of degassed aqueous 6 N NaOH. The golden solution was stirred in a 47 °C bath for 17 h. The solvent was removed by rotoevaporation, and the resulting yellow slurry was extracted with $CHCl_3$ (3 × 5 mL). The extract was washed with brine and dried (K_2CO_3). Evaporation of the solvent afforded 210 mg (90%) of **18** as a crystalline residue which resisted attempts at recrystallization: mp 85–87 °C; IR ($CHCl_3$) no C=O absorption; ESR ($CHCl_3$) three lines, a_N = 14.83 G; mass spectrum, *m/e* (relative intensity) 185.152 (100) (calcd for $C_9H_{18}N_3O$ 185.153), 112 (26), 111 (32), 87 (28), 75 (47), 74 (37), 73 (26), 72 (32), 64 (47), 61 (21), 60 (58), 48 (32), 47 (42), 46 (63).

pH Studies with 18. Buffer system I,[18] described above, was used for the pH studies with **18**. A 10.9 mM stock solution of **18** was prepared by dissolving 2 mg of **18** in 1 mL of H_2O. ESR samples, $\sim 10^{-4}$ M in **18**, were prepared by combining 10 μL of the stock solution with 990 μL of the appropriate buffer.

Vesicle Experiments with 18. A vial was charged with 83 mg of egg yolk lecithin, 2.5 mL of pH 2.2 citric acid buffer,[19] and 5 mg of **18**. The resulting mixture, 11 mM in **18**, was sonicated (N_2) in an ice bath for 30 min (40-W setting). The pH of the sonicate was 2.4. Half of the sonicate was placed (5 °C) on a 0.8 × 22 cm Sephadex G-25 coarse column which had been preequilibrated with pH 6.9 buffer. Elution with pH 6.9 buffer afforded, after about a 3-mL void volume, the turbid vesicle fraction (1.9 mL, pH 6.9). Continued elution with the same buffer afforded the pale yellow fractions containing untrapped **18**. The vesicle fraction was divided into several aliquots and stored on ice for the ESR experiments involving sodium ascorbate and $K_3Fe(CN)_6$. The ESR spectrum (see text) of a 40-μL aliquot was recorded at 0 °C, and then the sample was immediately treated with 10 μL of chilled sodium ascorbate stock solution (pH 6.8) (250 mg/mL of phosphate buffer). A similar series of experiments was performed by utilizing a stock solution of $K_3Fe(CN)_6$ (99 mg/mL of phosphate buffer).

Acknowledgment. This research was supported by Public Health Service Research Grants GM 27137 and 24951 from the National Institute of General Medical Sciences. We thank Mr. R. S. Norton for performing some of the preliminary experiments which led to this paper and Dr. G. Bruce Birrell for valuable advice concerning the vesicle experiments.

Registry No. 11, 80028-49-5; **12**, 80028-50-8; **13**, 80028-51-9; **14**, 80028-52-0; **15**, 80028-53-1; **16**, 80028-54-2; **17**, 80028-55-3; **18**, 80028-56-4; 1,2-diamino-2-methylpropane, 811-93-8; cyclohexanone, 108-94-1; *N*-benzoyl-4-piperidone, 24686-78-0.

Studies on Spin-Trapped Radicals in γ-Irradiated Aqueous Solutions of L-Alanylglycine and L-Alanyl-L-alanine by High-Performance Liquid Chromatography and ESR Spectroscopy

Fumio Moriya,* Keisuke Makino, Nobuhiro Suzuki, Souji Rokushika, and Hiroyuki Hatano

Contribution from the Department of Chemistry, Faculty of Science, Kyoto University, Sakyo-ku, Kyoto, 606 Japan. *Received June 8, 1981*

Abstract: Aqueous solutions of L-alanylglycine and L-alanyl-L-alanine were γ irradiated in the presence of a spin trap, 2-methyl-2-nitrosopropane. Stable spin adducts produced in the γ-irradiated solutions were analyzed by high-performance liquid chromatography and ESR spectroscopy. The following spin adducts were found and identified: *t*-BuN(O·)CH-(CH_3)CONHCH$_2$COO$^-$ (I), NH_3^+–*CH(CH_3)CONH–*CH(COO$^-$)N(O·)–*t*-Bu (II), and *t*-BuN(O·)CH$_2$CH(NH_3^+)–CONHCH$_2$COO$^-$ (III) from L-alanylglycine; *t*-BuN(O·)–*CH(CH_3)CONH–*CH(CH_3)COO$^-$ (IV), NH_3^+–*CH(CH_3)–CONH–*C(CH_3)(COO$^-$)N(O·)–*t*-Bu (V), NH_3^+CH(CH_3)CONHCH(COO$^-$)CH$_2$N(O·)–*t*-Bu (VI), and *t*-Bu–N(O·)–CH$_2$CH(NH_3^+)CONHCH(CH_3)COO$^-$ (VII) from L-alanyl-L-alanine. Each of spin adducts II, IV, and V was found as a pair of diastereomeric radicals, which revealed mutually different hyperfine splitting constants. The two diastereomeric pairs of spin adducts II and V were individually separated. It was demonstrated that ESR spectra of spin adducts II, III, and VI changed remarkably with pH through the acid-dissociation equilibria of the carboxyl or amino groups. The pK_a values for the dissociation have been determined to be 1.8 and 1.6 for the carboxyl groups of the pair of diastereomeric spin adducts II. The pK_{COOH} values are lower than that of alanylglycine because of the electron-withdrawing character of the nitroxyl group.

The spin-trapping method is one of the useful techniques for detection and identification of short-lived radicals in various reaction systems, by which short-lived radicals are converted into the fairly stable nitroxyl radicals (spin-trapped radicals or spin adducts) through reactions with spin traps such as nitroso or nitrone compounds.[1-3] For example, when 2-methyl-2-nitroso-

0002-7863/82/1504-0830$01.25/0

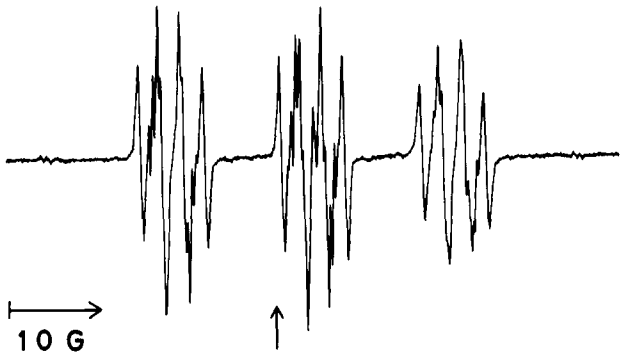

Figure 1. ESR spectrum of an aqueous solution of L-Ala-Gly with MNP observed just after γ irradiation (at pH 5.5). During chromatography the magnetic field was fixed at the position indicated by the vertical arrow.

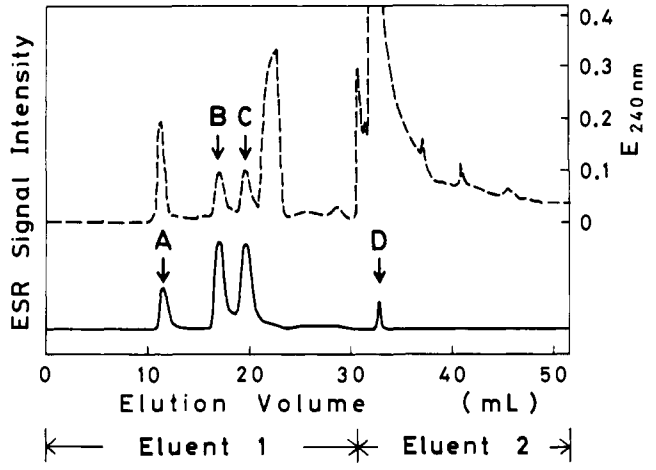

Figure 2. Chromatogram of the γ-irradiated aqueous solution of L-Ala-Gly with MNP drawn by UV (broken line) and ESR (solid line) detections: eluent 1, 0.15 M sodium phosphate buffer, pH 6.0; eluent 2, 0.2 M Na_2HPO_4–NaOH buffer, pH 11.5.

propane (MNP) is used as a spin trap, its reaction with short-lived radical (R·) is represented by eq 1.

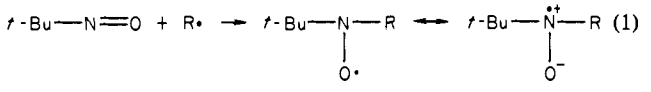

The spin-trapping method with MNP has been applied to γ- and UV-irradiated aqueous systems of peptides and proteins.[4-7] In most of these systems, the ESR spectra from irradiated solutions consisted of overlapped signals of several spin adducts. Liquid chromatography (LC) has recently been combined with ESR spectroscopy for the separation of radicals.[8] This technique has been applied to study spin adducts in the γ-irradiated aqueous systems of several nucleotides[9,10] and amino acids[11-14] with MNP as a spin trap and those in the γ-irradiated dry-powder systems of a few dipeptides.[15] The application of LC-ESR to γ radiolysis of MNP in an aqueous solution has also been reported.[16]

In a previous paper[17] we have reported several spin adducts in the γ-irradiated aqueous solutions of Gly-Gly and Gly-L-Ala with MNP at pH $\simeq$ 5.5. And the γ-radiolytic and spin-trapping mechanisms shown in eq 2–4 for dipeptides were proposed, where

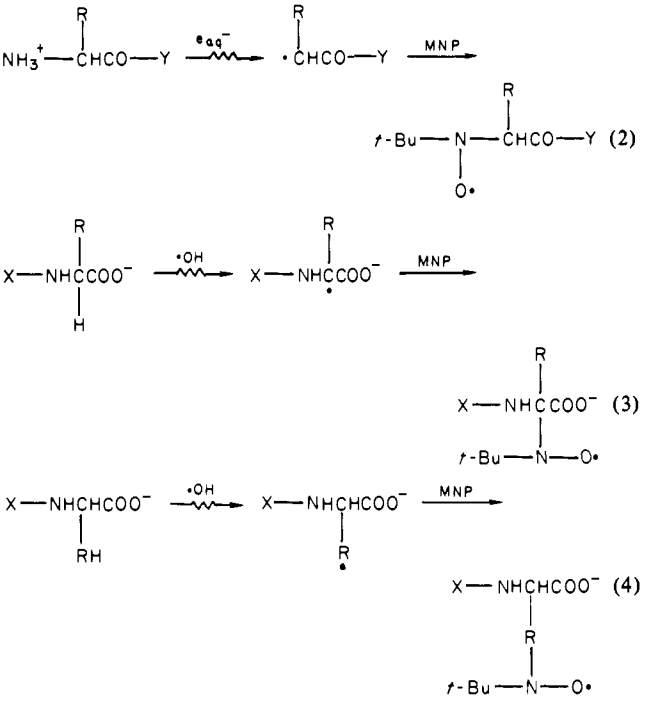

X and Y represent amino acid residues, R is H or a side chain, RH is an aliphatic side chain, and the left, central, and right members of each equation are a dipeptide, a short-lived radical, and a spin adduct, respectively. The spin adduct in eq 2 is derived from a deaminated radical produced by the addition of e_{aq}^- to the peptide carbonyl group.[18,19] The spin adducts in eq 3 and 4 are derived from radicals produced by hydrogen abstractions from a so-called α-carbon in the C-terminal main chain and a carbon in an aliphatic side chain, respectively, by ·OH mainly. The spin adducts in eq 2–4 were called a deamino adduct, a backbone adduct, and a side-chain adduct, respectively.

In the present work, the spin-trapping method with MNP was applied to γ-irradiated aqueous solutions of L-Ala-Gly and L-Ala-L-Ala. All of the spin adducts expected from eq 2–4 which involve diastereomers were found and characterized by high-performance liquid chromatography (HPLC) and ESR spectroscopy.

Experimental Section

L-Ala-Gly and L-Ala-L-Ala were purchased from Sigma Chemical Co., Saint Louis, MO. MNP was synthesized and purified according to the method of Stowell.[20] All other chemicals were of reagent grade.

(1) Janzen, E. G. *Acc. Chem. Res.* **1971**, *4*, 31–40 and references therein.
(2) Lagercrantz, C. *J. Phys. Chem.* **1971**, *75*, 3466–3475 and references therein.
(3) Evans, C. A. *Aldrichimica Acta* **1979**, *12*, 23–29 and references therein.
(4) Taniguchi, H.; Hatano, H. *Chem. Lett.* **1974**, 531–534; **1975**, 9–12.
(5) Joshi, A.; Rustgi, S.; Moss, H.; Riesz, P. *Int. J. Radiat. Biol. Relat. Stud. Phys., Chem. Med.* **1978**, *33*, 205–229.
(6) Rustgi, S.; Riesz, P. *Int. J. Radiat. Biol. Relat. Stud. Phys., Chem. Med.* **1978**, *34*, 127–148, 449–460.
(7) Riesz, P.; Rustgi, S. *Radiat. Phys. Chem.* **1979**, *13*, 21–40 and references therein.
(8) Rokushika, S.; Taniguchi, H.; Hatano, H. *Anal. Lett.* **1975**, *8*, 205–213.
(9) Kominami, S.; Rokushika, S.; Hatano, H. *Int. J. Radiat. Biol. Relat. Stud. Phys., Chem. Med.* **1976**, *30*, 525–534.
(10) Kominami, S.; Rokushika, S.; Hatano, H. *Radiat. Res.* **1977**, *72*, 89–99.
(11) Makino, K.; Hatano, H. *Chem. Lett.* **1979**, 119–122.
(12) Makino, K.; Suzuki, N.; Moriya, F.; Rokushika, S.; Hatano, H. *Anal. Lett.* **1980**, *13*, 301–309.
(13) Makino, K. *J. Phys. Chem.* **1979**, *83*, 2520–2523; **1980**, *84*, 1016–1019, 1968–1974.
(14) Moriya, F.; Makino, K.; Suzuki, N.; Rokushika, S.; Hatano, H. *J. Phys. Chem.* **1980**, *84*, 3085–3090.
(15) Minegishi, A.; Bergene, R.; Riesz, P. *Int. J. Radiat. Biol. Relat. Stud. Phys., Chem. Med.* **1980**, *38*, 627–650.
(16) Makino, K.; Suzuki, N.; Moriya, F.; Rokushika, S.; Hatano, H. *Chem. Lett.* **1979**, 675–678. Makino, K. *J. Phys. Chem.* **1980**, *84*, 1012–1015.
(17) Moriya, F.; Makino, K.; Suzuki, N.; Rokushika, S.; Hatano, H. *J. Phys. Chem.* **1980**, *84*, 3614–3619.
(18) Willix, R. L. S.; Garrison, W. M. *Radiat. Res.* **1967**, *32*, 452–462.
(19) Klapper, M. H.; Faraggi, M. *Q. Rev. Biophys.* **1979**, *12*, 465–519 and references therein.

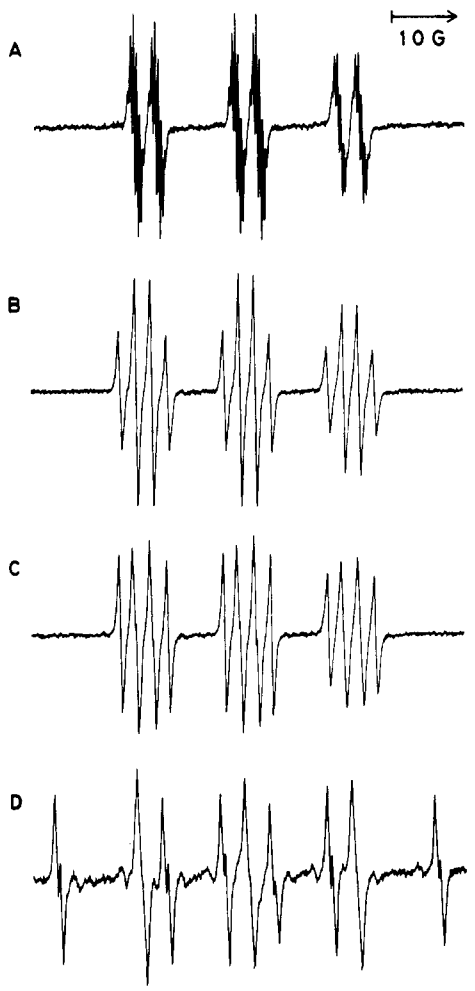

Figure 3. ESR spectra of the separated spin adducts. A–D represent the spectra obtained from the fractions giving peaks A–D in Figure 2, respectively: A–C, pH 6.0; D, pH 8.0.

The dipeptides (0.1 M) were dissolved into 5 mg/mL of MNP aqueous solutions.[21] The sample solution was cooled by ice and irradiated with ^{60}Co γ-rays at a dose rate of 6.0×10^5 rad/h to a total dose of 3.0×10^5 rad without deaeration. The concentration of phosphoric ion in the irradiated solution was adjusted to 0.15 M by 2 M sodium phosphate, and 1.0 mL of the solution was added to a 0.75 × 60 cm cation-exchange column (IEX-210SC of Toyo Soda Manufacturing Co., Tokyo, Japan). The HPLC was a Toyo Soda HLC-803. The eluate was passed through UV and ESR detectors and collected into fraction tubes. The UV detector was tuned to 240 nm. The ESR spectrometer was a JEOL PE-3X, which was operated at 100-kHz modulation frequency in the X-band. For detection of the radicals during chromatography, the magnetic field was fixed at the positions indicated by the vertical arrows in Figures 1 and 6. The magnetic field modulation was used at a high amplitude of 10 G to cover a wide range. A quartz flow cell (the practical part being the 0.6-mm i.d. and 5-cm length) was fixed in the ESR cavity. Each of parts in the chromatographic system was connected with 0.25-mm i.d. Teflon tubing. The conditions of the chromatography were as follows: pressure, ca. 70 kg/cm^2; flow rate, ca. 0.2 mL/min; temperature, ca. 25 °C.

The ESR spectra were recorded at ca. 25 °C in the dark. Some of the fractions were mildly bubbled with nitrogen gas for ca. 1 min to prevent a lowering of the ESR spectral resolution due to dissolved molecular oxygen. Hyperfine splitting constants (hfsc's) were measured by using Mn^{2+} in MgO as a reference. The simulation of the ESR spectra was achieved with Lorentzian peak-to-peak line widths by using a JEOL JEC-980A minicomputer. The pH of the solutions was adjusted with dilute HCl or NaOH. Ninhydrin-positive fractions were analyzed by an amino acid analyzer (Hitachi KLA-3B).

For other experimental details refer to our previous work.[17]

(20) Stowell, J. C. *J. Org. Chem.* **1971**, *36*, 3055–3056.
(21) Makino, K.; Suzuki, N.; Moriya, F.; Rokushika, S.; Hatano, H. *Anal. Lett.* **1980**, *13*, 311–317; *Radiat. Res.* **1981**, *86*, 294–310.

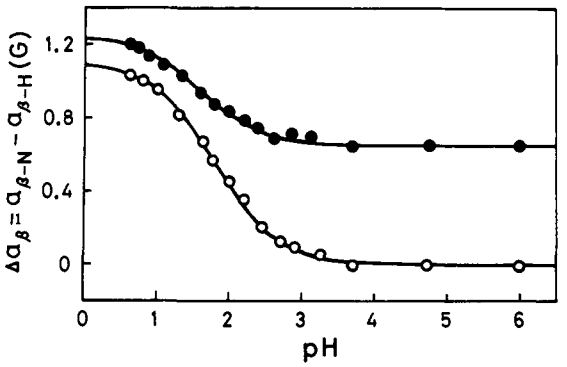

Figure 4. The effect of pH on the differences in the β hfsc's for spin adducts IIa (○) and IIb (●). Best-fitted solid lines were calculated by use of eq 5.

Results and Interpretations

L-Alanylglycine. Figure 1 shows the ESR spectrum of a γ-irradiated aqueous L-Ala-Gly solution with MNP. The chromatogram of the solution by UV and ESR detections is shown in Figure 2. The ESR chromatogram exhibited four peaks (A–D) as shown by the solid line. Typical ESR spectra for the fractions of peaks A–D are depicted in Figure 3A–D, respectively. Most of spin adducts produced by the self-trapping of MNP[16] were adsorbed on the column and eluted very slowly. In the UV chromatogram shown by the broken line in Figure 2, the fourth peak was due to intact L-Ala-Gly and the large peak containing peak D by ESR detection was mainly due to *tert*-butylnitrosohydroxylamine (*t*-BuN(OH)N=O).[21]

Figure 3A shows the ESR spectrum obtained for the peak A fraction, which can be analyzed as a triplet–doublet–sextet. The primary triplet of 15.8-G splitting is due to the nitrogen nucleus in the nitroxyl group, and the secondary doublet of 3.3-G splitting is due to a β-hydrogen nucleus. The spin adduct was assigned to structure I, the deamino adduct from L-Ala-Gly, on the basis

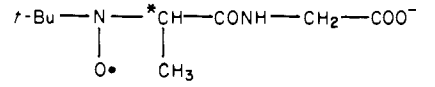

I

of its hyperfine structure (hfs) and elution position. The fine sextet of equally spaced splitting was interpreted as that with an intensity ratio of 1:4:7:7:4:1 which originates from a γ-nitrogen in the peptide bond and three equivalent γ-hydrogens in the methyl group of the L-alanine side chain ($a_{\gamma\text{-N}} = a_{\gamma\text{-H}} = 0.47$ G).

Parts B and C of Figure 3 show the ESR spectra for the fractions of peaks B and C, respectively, which are similar to but not identical with each other and are apparently major components of ESR signals in Figure 1. The secondary hfs of each spectrum is due to a β-hydrogen and a β-nitrogen. Both spin adducts were assigned to structure II, the backbone adduct from L-Ala-Gly.

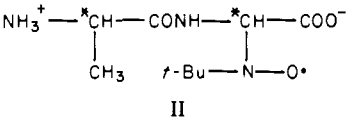

II

The ESR spectra resemble that of the backbone adduct from Gly-Gly.[17] The adducts of peaks B and C are interpreted as a pair of diastereomeric radicals,[12,22] S–S and S–R forms, by the primary asymmetric center of the L-alanine residue and the new asymmetric center formed by the addition of MNP to the short-lived radical. The adduct of peak B ($a_N = 15.5$ G, $a_{\beta\text{-H}} = a_{\beta\text{-N}} = 2.33$ G at pH 6.0) refers to structure IIa and that of peak C ($a_N = 15.6$ G, $a_{\beta\text{-H}} = 1.93$ G, $a_{\beta\text{-N}} = 2.58$ G at pH 6.0) to IIb. Both isomers exhibited little spectral changes in the neutral and alkaline pH range. However, in the acidic pH range they exhibited

(22) Jonkman, L.; Muller, H.; Kommandeur, J. *J. Am. Chem. Soc.* **1971**, *93*, 5833–5838.

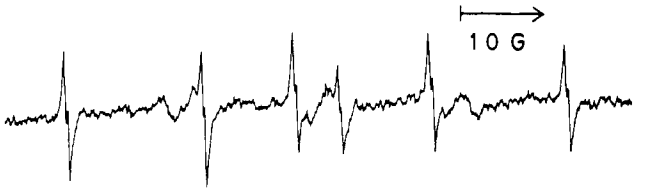

Figure 5. ESR spectrum of spin adduct III observed at pH 2.0.

reversible pH-dependent shifts of their signals. Their hfsc's at pH 0.8 are given in Table II later. The spectral changes of the respective isomers are mainly due to an increase of the differences in the β hfsc's and are caused by the acid-dissociation equilibrium of the carboxyl groups in the vicinity of the nitroxyl groups. The differences in the β hfsc's, $\Delta a_\beta = a_{\beta\text{-N}} - a_{\beta\text{-H}}$, were plotted as functions of pH in Figure 4. Since the interchange between the acid form (A) and the base form (B) is rapid in the equilibrium, the observed Δa_β represents the weighted average of the two forms with $\Delta a_\beta^{\text{A}}$ and $\Delta a_\beta^{\text{B}}$, respectively.[23,24] For a given solution Δa_β is derived as a function of pH in eq 5,[17] where $\Delta a_\beta^{\text{A}} = 1.10$ G

$$\Delta a_\beta = \frac{\Delta a_\beta^{\text{A}} + \Delta a_\beta^{\text{B}} \times 10^{\text{pH}-\text{p}K_a}}{1 + 10^{\text{pH}-\text{p}K_a}} \qquad (5)$$

and $\Delta a_\beta^{\text{B}} = 0$ for adduct IIa and $\Delta a_\beta^{\text{A}} = 1.25$ G and $\Delta a_\beta^{\text{B}} = 0.65$ G for IIb. The best fits for the experimental points were obtained by substituting $\text{p}K_a = 1.8$ for adduct IIa and 1.6 for IIb in eq 5, as shown by the solid lines in Figure 4. The measurement of the optical rotations at 411 nm revealed that spin adduct IIa is dextrorotatory at pH 6.0. The optical rotatory power of adduct IIb could not be determined, owing to considerable contamination with intact L-Ala-Gly eluted just after peak C.

Figure 3D shows the ESR spectrum for the peak D fraction, which apparently exhibits a mixture of six narrow and three broad lines. Each of the nine lines further splits into a small doublet. Since the narrow set and the broad set gave the same g value and N-hfsc, the spectrum was inferred to be due to only one kind of spin adduct with line-width alternation (LWA). It can be analyzed as three groups of a 1:2:1 triplet whose central signal is selectively broad. The primary N-hfsc is 16.5 G, and the secondary splittings were assigned to two equivalent β-hydrogens and a γ-hydrogen ($a_{\beta\text{-H}} = 12.6$ G, $a_{\gamma\text{-H}} = 0.7$ G at pH 8.0). The observed spectrum (Figure 3D) was well consistent with a simulated one which was computed with line widths of 0.5 and 0.7 G by considering that the peak-to-peak derivative amplitude is inversely proportional to the square of the line widths when ESR signals with equal intensities belong to an identical type of line shape.[25] The spin adduct was assigned to structure III, the side-chain adduct from L-Ala-Gly. The two β-hydrogens of spin adduct III gave equivalent

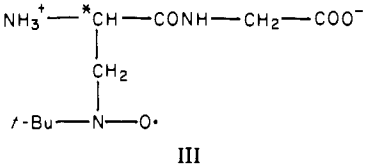

III

hyperfine splittings in the alkaline range above pH 8, whereas at pH 5.9 the central broad lines of 1:2:1 triplets due to the β-hydrogens disappeared. Figure 5 shows the ESR spectrum observed at pH 2.0 ($a_{\text{N}} = 16.2$ G, $a_{\beta\text{-H}} = 15.3$ and 11.8 G, $a_{\gamma\text{-H}} = 0.5$ G), which is a typical pattern for a *tert*-butylnitroxyl radical which has an α-methylene and an asymmetric β-carbon in the molecule, that is, t-Bu—N(O·)—CH_2—*CXYZ. The characteristic nonequivalence of the two β-hydrogens with LWA was interpreted by assuming, for example, insufficient rapid interconversion between two rotamers which have mutually different sets of β-H hfsc's.[26]

(23) Neta, P. *Adv. Phys. Org. Chem.* **1975**, *12*, 223–297.
(24) Kirino, Y. *J. Phys. Chem.* **1975**, *79*, 1296–1300.
(25) Wertz, J. E.; Bolton, J. R. "Electron Spin Resonance. Elementary Theory and Practical Applications"; McGraw-Hill: New York, 1972; pp 32–36.

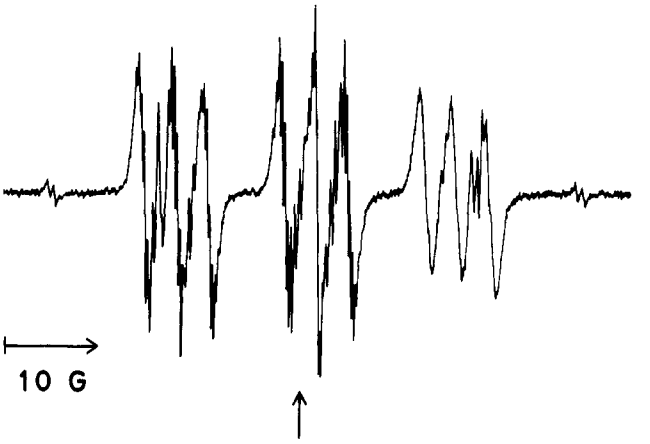

Figure 6. ESR spectrum of an aqueous solution of L-Ala-L-Ala with MNP observed just after γ irradiation (at pH 5.5). During chromatography the magnetic field was fixed at the position indicated by the vertical arrow.

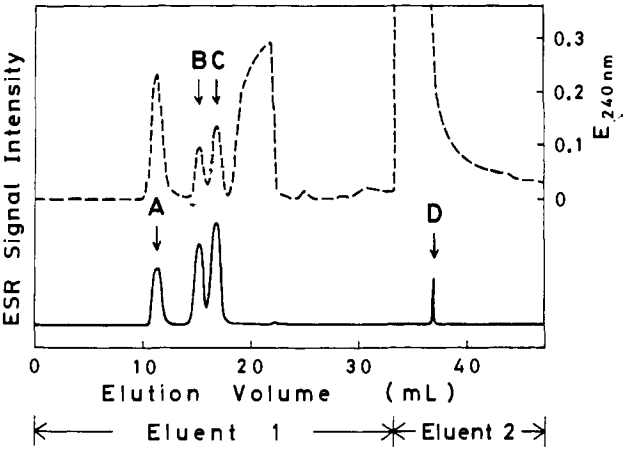

Figure 7. Chromatogram of the γ-irradiated aqueous solution of L-Ala-L-Ala with MNP drawn by UV (broken line) and ESR (solid line) detections: eluent 1, 0.15 M sodium phosphate buffer, pH 6.0; eluent 2, 0.2 M Na_2HPO_4–NaOH buffer, pH 11.5.

L-Alanyl-D-alanine. Figures 6 and 7 show the ESR spectrum and the chromatogram of a γ-irradiated aqueous L-Ala-L-Ala solution with MNP, respectively. The ESR chromatogram exhibited four peaks (A–D) as shown by the solid line in Figure 7. Typical ESR spectra for the fractions of peaks A–D are depicted in Figure 8A–D, respectively. In the UV chromatogram shown by the broken line in Figure 7, the fourth peak was due to intact L-Ala-L-Ala and the large fifth peak was mainly due to t-BuN(OH)NO.[21]

The ESR spectrum of the peak A fraction (Figure 8A) was assigned to the deamino adduct from L-Ala-L-Ala, that is

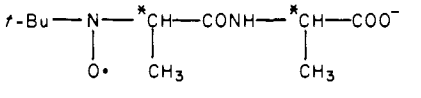

IV

Each block of the triplet–doublet splittings of spin adduct IV exhibited asymmetry with distortions as shown clearly in Figure 9A while adduct I gave symmetrical blocks (Figure 3A). This fact suggests the coexistence of a pair of diastereomeric adducts, S–S and R–S forms, ascribed to a new asymmetric center which results from the spin-trapping process of a short-lived deamino radical from L-Ala-L-Ala. Computer simulation for the ESR spectrum was conducted by assuming that the fraction is an equivalent mixture of two kinds of radicals whose ESR parameters

(26) Gilbert, B. C.; Trenwith, M. *J. Chem. Soc., Perkin Trans. 2* **1973**, 1834–1839.

Table I. Parameters (G) Used for the Simulated Spectrum in Figure 9B

isomer[a]	hfsc a_N	hfsc $a_{\beta\text{-H}}$	hfsc $a_{\gamma\text{-H}}$ (3 H)	hfsc $a_{\gamma\text{-N}}$	center of spectrum	peak-to-peak line width[b] M_I component +1	M_I component 0	M_I component −1
IVa	15.75	3.85	0.45	0.45	H_0	0.30	0.30	0.35
IVb	15.80	3.65	0.50	0.50	H_0 + 0.025	0.30	0.30	0.35

[a] Calculated with a concentration ratio of 1:1 for these diastereomeric isomers. [b] With the assumption of Lorentzian line shape.

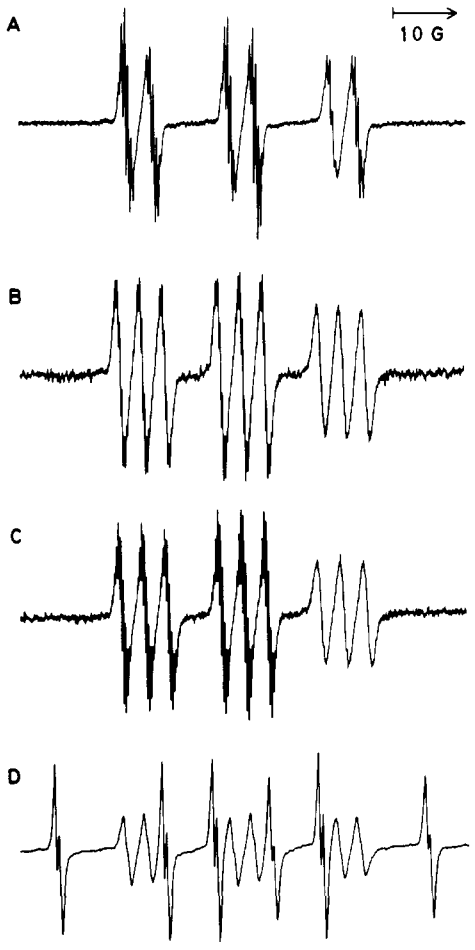

Figure 8. ESR spectra of the separated spin adducts. A–D represent the spectra obtained from the fractions giving peaks A–D in Figure 7, respectively: A–C, pH 6.0; D, pH 9.0.

are slightly distinct from each other. The resulting spectrum from the calculation using the parameters summarized in Table I is shown in Figure 9B and is in good agreement with the observed one.

Parts B and C of Figure 8 show the ESR spectra for the fractions of peaks B and C, respectively, which are apparently the major components of the ESR signals in Figure 6. These spin adducts which gave mutually similar triplet–triplet splittings with equal signal intensities were assigned to a pair of the diastereomeric backbone adducts (S–S and S–R forms), that is

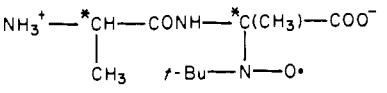

V

It has been proved by thorough examination that spin adducts of peaks B and C give ESR spectra different from each other. The enlarged spectra of the $M_I = 0$ components of adducts Va (peak B) and Vb (peak C) and their simulated spectra are shown in Figure 10. The ESR parameters of the computer simulation were as follows: 0.32-G line widths, $a_{\beta\text{-N}}$ = 3.39 G and $a_{\gamma\text{-H}}$ (10 H) = 0.34 G for adduct Va (Figure 10A, observed; 10B, simulated); 0.25-G line widths, $a_{\beta\text{-N}}$ = 3.50 G, $a_{\gamma\text{-H}}$ (13 H) = 0.32 G

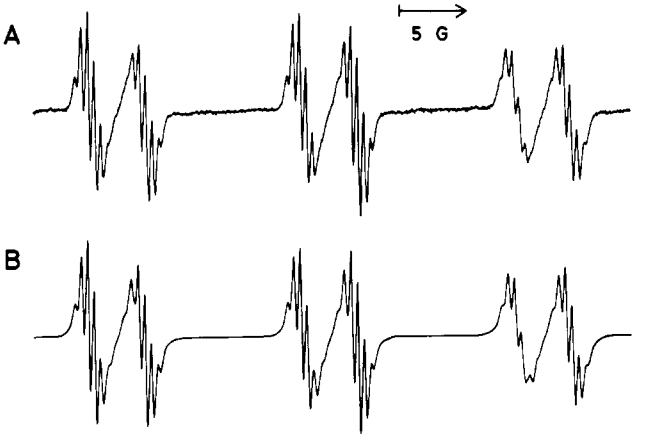

Figure 9. (A) Enlarged ESR spectrum of Figure 8A. (B) Computer-simulated spectrum for A. Parameters used for spectrum simulation are specified in Table I.

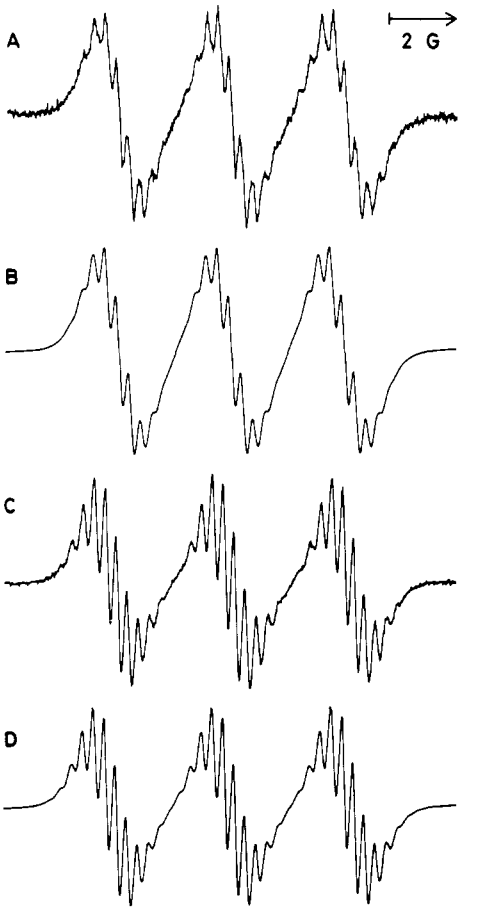

Figure 10. (A and C) Enlarged ESR spectra of the $M_I = 0$ components in parts B and C of Figure 8. (B and D) Computer-simulated spectra for A and C, respectively. Parameters used for spectrum simulation are specified in the text.

for adduct Vb (Figure 10C, observed; 10D, simulated). It was revealed that the γ hfs of spin adduct Vb consists of all 13 γ-hydrogens while that of Va lacks three hydrogens in the C-terminal

Table II. Hyperfine Splitting Constants (G) of Spin Adducts from Dipeptides

substrate	structure[a]		pH	a_N	$a_{\beta\text{-H}}$	$a_{\beta\text{-N}}$	$a_{\gamma\text{-H}}$	$a_{\gamma\text{-N}}$
	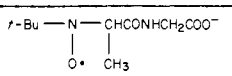	I	6.0	15.8	3.3		0.47[b]	0.47
L-Ala-Gly	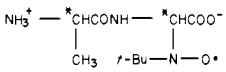	IIa	11.2	15.7	2.15	2.35		
			6.0	15.5	2.33	2.33		
			0.8	15.2	1.60	2.60		
		IIb	11.3	15.8	2.05	2.45		
			6.0	15.6	1.93	2.58		
			0.8	15.3	1.50	2.70		
	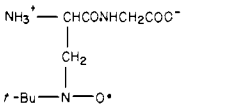	III	8.0	16.5	12.6[c]		0.7	
			5.9	16.2	*d*		0.5	
			2.0	16.2	15.3, 11.8		0.5	
	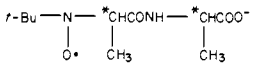	IVa	6.0	15.75	3.85		0.45[b]	0.45
		IVb	6.0	15.80	3.65		0.50[b]	0.50
	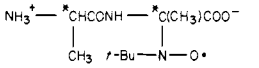	Va	6.0	15.3		3.39	0.34[e]	
		Vb	6.0	15.2		3.50	0.32[f]	
L-Ala-L-Ala	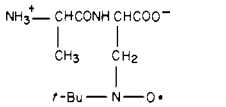	VI	12.4	16.3	13.6, 10.5		0.7	
			7.9	16.4	14.0, 10.1		0.7	
			6.1	16.4	14.3, 9.9		0.7	
			1.0	16.5	13.9[c]		0.7	
	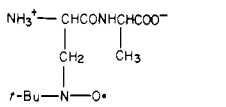	VII	7.9	16.5	12.8[c]		0.7	

[a] Shown as structures at pH 6. [b] Three equivalent hydrogens. [c] Two equivalent hydrogens. [d] The two β-hydrogens were presumably nonequivalent ($\Sigma a_{\beta\text{-H}}$ = 26.3 G). [e] Ten equivalent hydrogens. [f] Thirteen equivalent hydrogens.

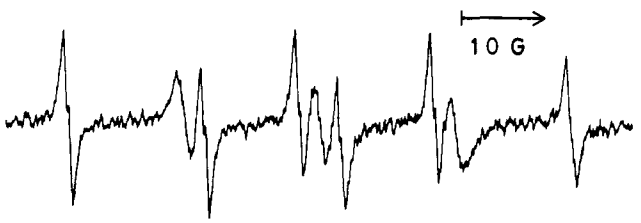

Figure 11. ESR spectrum of spin adduct VI observed at pH 1.0.

L-alanine side-chain to consist of 10 equivalent γ-hydrogens.

Figure 8D shows the ESR spectrum for the peak D fraction, which is a typical pattern of a nitroxyl radical, *t*-Bu—N(O·)—CH_2—*CXYZ.[26] The hfsc's at pH 9.0 are as follows: a_N = 16.3 G, $a_{\beta\text{-H}}$(2 H) = 13.7 and 10.4 G, and $a_{\gamma\text{-H}}$ = 0.7 G. The spin adduct exhibited reversible spectral changes accompanying pH variation. In the pH range above ca. 4 the nonequivalent β-H hfs pattern was held, and the spectral changes around pH 8 were relatively small. The hfsc's at pH 6.1, 7.9, and 12.4 are given in Table II. Around pH 3 remarkable spectral changes were observed with pH-dependent broadening and shifts of the signals. Figure 11 shows the ESR spectrum observed at pH 1.0, where the β-hydrogens gave equal hfsc's of 13.9 G with LWA. As described above the spectral behavior of this spin adduct is very similar to that of the side-chain adduct from Gly-L-Ala[17] and is not similar to that of adduct III from L-Ala-Gly. Therefore, this adduct was assigned to the C-terminal side-chain adduct (structure VI).

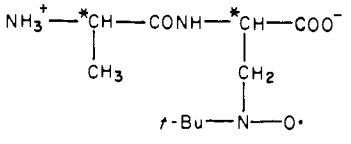

VI

No other significant spin adducts were detected from the chromatographic result which was carried out with the same condition shown in Figure 7. However, when the sodium phosphate buffers of 0.05 M, pH 6.0, and 0.1 M, pH 8.0, were used as the first and the second eluents, respectively, the ESR spectrum shown in Figure 12A was observed for the fraction in the position where the pH value of the eluate rose to 7.9. The computer simulation of the spectrum was performed by assuming that the fraction consists of two species. One of them is adduct VI with line widths of 0.5 and 0.9 G, and the other is a newly detected adduct. Consequently the simulated spectrum shown in Figure 12B was obtained by computing with the following conditions: for the new adduct a_N = 16.5 G, $a_{\beta\text{-H}}$(2 H) = 12.8 G, and $a_{\gamma\text{-H}}$ = 0.7 G and line widths of the β-H triplet with an intensity ratio of 1:2:1 are 0.5, 0.9, and 0.5 G, respectively; the concentration ratio of this adduct to adduct VI is 1:2 and they have the same *g* value. The simulated ESR spectrum for the new adduct is shown in Figure 12C. The equivalent hfs pattern of the two β-hydrogens with LWA in the alkaline pH range is consistent with the case of spin adduct III from L-Ala-Gly. The new adduct was assigned to the N-terminal side-chain adduct (structure VII).

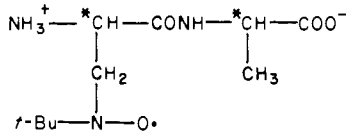

VII

The structures and hfsc's of the spin adducts in the γ-irradiated aqueous solutions of L-Ala-Gly and L-Ala-L-Ala with MNP are summarized in Table II.

Discussion

Here we wish to discuss the results obtained from the γ-radiolytic aqueous systems of the four dipeptides including Gly-Gly and Gly-L-Ala which were reported previously.[17]

Production of Spin Adducts in γ-Irradiated Aqueous Solutions of Dipeptides. All of the spin adducts expected from eq 2–4 were found, that is, primary deamino adducts originated from attacks of hydrated electrons and C-terminal backbone adducts and side-chain adducts derived from hydrogen abstractions by hydroxyl radicals mainly. This fact indicates that most of short-lived

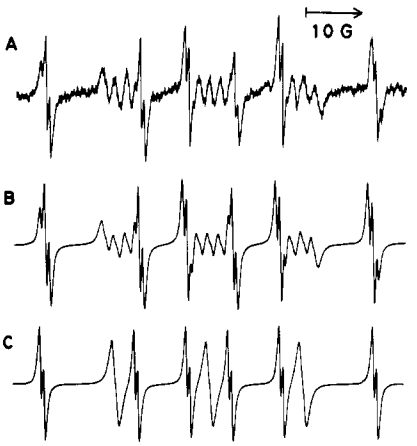

Figure 12. (A) ESR spectrum obtained from the pH 7.9 fraction given under an elution condition different from that shown in Figure 7. (B) Computer-simulated spectrum for A. The concentration ratio for spin adduct VI and a newly detected spin adduct was assumed as 2:1. (C) Calculated spectrum of the new adduct. The elution condition and parameters used for spectrum simulation are specified in the text.

radicals previously found in aqueous solutions of the dipeptides[27-31] are spin trapped.

In previous papers,[18,32] Garrison et al. reported that the ·OH attacks Gly-Gly at the α-position to the peptide nitrogen and not to the NH_3^+ group. Hydrogen abstraction by ·OH at the α-position to the peptide nitrogen was observed by pulse radiolysis,[33] UV photolysis with H_2O_2,[30] and the Ti^{3+}–H_2O_2 method.[34] The main production of C-terminal backbone adducts in the present work is compatible with the previous conclusion. N-Terminal backbone adducts such as *t*-BuN(O·)–$CH(NH_3^+)CONHCH(CH_3)COO^-$ from Gly-L-Ala were not ascertained.

The second-order rate constants for reactions between e_{aq}^- and amino acids or peptides were previously determined by pulse radiolysis.[19,35] The rate constants at pH 5.9–6.4 were (5.9–8.3) × 10^6 M^{-1} s^{-1} for glycine and α-alanine and (1.3–3.7) × 10^8 M^{-1} s^{-1} for dipeptides made up of the amino acids, which suggests that an e_{aq}^- attack on a peptide carbonyl group is much faster than that on a carboxyl group. Therefore, it is reasonable that "secondary deamino adducts" originating from attacks of e_{aq}^- on carboxyl groups such as *t*-BuN(O·)CH_2COO^- from L-Ala-Gly were not found in our present work.

"Decarboxyl adducts" such as $NH_3^+CH_2CONHCH(CH_3)$–N(O·)–*t*-Bu from Gly-L-Ala were not ascertained also.

The pH Dependence of ESR Spectra of the Spin Adducts and the pK_a Values of Their Proton Dissociation Groups. Most spin adducts exhibited pH-dependent reversible changes in ESR spectra through the acid-dissociation equilibria of the carboxyl or amino groups in proximity to the nitroxyl groups. For several of the spin adducts whose spectra changed remarkably, acid-dissociation constants were determined by appropriate procedures. The pK_{COOH} values have been determined to be 3.2, 2.0, 1.8, and 1.6 for *t*-BuN(O·)$CH(CH_3)COOH$,[14] $NH_3^+CH_2CONHCH$-(COOH)N(O·)—*t*-Bu,[17] adduct IIa, and adduct IIb, respectively. It appears from the electron-withdrawing character of the nitroxyl group that the pK_{COOH} values are lower than those of the compounds in which the *tert*-butylnitroxyl groups of the adducts are substituted by hydrogens.

In each of the C-terminal side-chain adducts from Gly-L-Ala[17] and L-Ala-L-Ala in the acidic pH range and the N-terminal side-chain adducts from L-Ala-Gly and L-Ala-L-Ala in the alkaline pH range, the two β-hydrogens give equivalent hfsc's maintaining LWA. The results suggest that, when no electric charges exist in close vicinity to the β asymmetric center, its asymmetric effect on the β-hydrogens is too small to make their hfsc's nonequivalent. Alternatively, in an aqueous solution the function of the β asymmetric center that makes the methylene hydrogens nonequivalent[26] seems to be enhanced by electric charges in proximity to the center.

Registry No. I, 79919-30-5; IIa, 79919-31-6; IIb, 79919-32-7; III, 79919-33-8; IVa, 79919-34-9; IVb, 79919-35-0; Va, 79919-36-1; Vb, 79919-37-2; VI, 79919-38-3; VII, 79919-39-4; L-Ala-Gly, 687-69-4; L-Ala-L-Ala, 1948-31-8; MNP, 917-95-3.

(27) Neta, P.; Fessenden, R. W. *J. Phys. Chem.* **1970**, *74*, 2263–2266.
(28) Sevilla, M. D. *J. Phys. Chem.* **1970**, *74*, 3366–3372.
(29) Sevilla, M. D.; Brooks, V. L. *J. Phys. Chem.* **1973**, *77*, 2954–2959.
(30) Livingston, R.; Doherty, D. G.; Zeldes, H. *J. Am. Chem. Soc.* **1975**, *97*, 3198–3204.
(31) Sevilla, M. D.; D'Arcy, J. B.; Morehouse, K. M. *J. Phys. Chem.* **1979**, *83*, 2887–2892.
(32) Garrison, W. M. *Radiat. Res. Rev.* **1972**, *3*, 305–326.
(33) Hayon, E.; Ibata, T.; Lichtin, N. N.; Simic, M. *J. Am. Chem. Soc.* **1970**, *92*, 3898–3903; **1971**, *93*, 5388–5394.
(34) Taniguchi, H.; Hatano, H.; Hasegawa, H.; Maruyama, T. *J. Phys. Chem.* **1970**, *74*, 3063–3065.
(35) Anbar, M.; Bambenek, M.; Ross, A. B. *Natl. Stand. Ref. Data Ser. (U.S., Natl. Bur. Stand.)* **1973**, *43*. Ross, A. B. *Ibid.* **1975**, *43* (supplement).